

Cosmic microwave background anisotropy from wiggly strings

Levon Pogosian and Tanmay Vachaspati

Physics Department, Case Western Reserve University, Cleveland, Ohio 44106-7079

(Received 25 March 1999; published 8 September 1999)

We investigate the effect of wiggly cosmic strings on the cosmic microwave background radiation anisotropy and matter power spectrum by modifying the string network model used by Albrecht *et al.* We employ the wiggly equation of state for strings and the one-scale model for the cosmological evolution of certain network characteristics. For the same choice of simulation parameters we compare the results with and without including wiggleness in the model and find that wiggleness together with the accompanying low string velocities leads to a significant peak in the microwave background anisotropy and to an enhancement in the matter power spectrum. For the cosmologies we have investigated (standard CDM and CDM plus a cosmological constant), and within the limitations of our modeling of the string network, the anisotropy is in reasonable agreement with current observations but the COBE normalized amplitude of density perturbations is lower than what the data suggest. In the case of a cosmological constant and CDM model, a bias factor of about 2 is required. [S0556-2821(99)05518-6]

PACS number(s): 98.80.Cq

I. INTRODUCTION

The origin of the large-scale structure of the Universe has been a focus of active research for the last few decades and is still one of the major unresolved problems in cosmology. Measurements of the anisotropy in the cosmic microwave background radiation (CMBR) have inspired hope that different theories of structure formation can be tested observationally. Quantum fluctuations in inflationary models and topological defects are two important sources of density inhomogeneities that would have different imprints on the CMBR and which one could hope to distinguish.

Cosmic strings are a special variety of topological defects that have been studied in the context of seeding large-scale structure. Rapid progress on both observational and theoretical issues has resulted in more accurate estimates of the CMBR anisotropy due to strings [1–6]. The existence of publicly available computer codes [7] that can determine the anisotropy for given matter energy-momentum tensors has greatly facilitated the study of mechanisms that can source the CMBR anisotropy.

The major hurdle in calculating the effect of strings on the CMBR is that there is no simple way to characterize the network of strings. Large scale computer simulations have provided insight into some of the properties of the network [8] within some choice of background cosmologies. However, there are still unknown characteristics that could be important for predictions of the CMBR anisotropy and the large-scale power spectrum. As a result, certain extrapolations have to be made to characterize the string network in the regime where details are not yet available. This “network modeling” is the crucial aspect of analyzing the observable signatures of cosmic strings.

Over the last decade or so, a number of approaches have been taken to determine the detailed imprint of cosmic strings on the CMBR. The first attempt in this direction worked directly with the network of strings found in computer simulations [9]. Recently, this numerical analysis has been refined and extended [10]. The drawback in any such

numerical attempt is that the dynamic range of the simulations cannot yet extend to cover a cosmic expansion factor of at least 10^4 . It appears that some network modeling is essential as was first attempted in [11]. In recent work [4] the CMBR anisotropy was calculated using the results of a lattice simulation of a string network in a flat spacetime background. Another approach, first suggested in [12] and further developed in [2,3], approximates the string network by a collection of randomly oriented straight string segments, moving with random velocities. This model has the merit of being relatively simple and amenable to modifications that seem to be indicated by direct simulations. Hence, we have adopted this model and, for the first time, included small-scale structure on the string segments. Furthermore, we have modeled the parameters of the segments (length, velocity, wiggleness) by using the “one-scale model” of cosmic string networks [13,14] and some reasonable expectations of how the strings would behave in an inflating background.

The most important feature that we have taken into account in modeling the string network is the presence of small-scale structure on the strings. The scale of the wiggles is much smaller than the characteristic length of the string. In fact, a distant observer will not be able to resolve the details of the wiggly structure. Instead, she would see a smooth string, but the string would possess somewhat different characteristics. For a string with no wiggles, the equation of state is $\mu = T = \mu_0$, where μ is the effective mass per unit length and T is the tension of the string. A wiggly string, however, has a different effective equation of state [15,16]:

$$\mu T = \mu_0^2, \quad \mu > T.$$

The wiggly string is heavier and slower than a Nambu-Goto string.

The perturbation in the metric produced by a wiggly string is similar to that of a smooth string. As was shown in [17], in both cases, the space in the vicinity of a straight segment of a string is conical with a deficit angle $\Delta = 8\pi G\mu$. The deficit angle is larger for wiggly strings, since

they have a larger effective mass per unit length. However, a new important feature of the wiggly string metric is a non-zero Newtonian potential $\phi \propto (\mu - T)$. (So the wiggly string behaves as a superposition of a massive rod and a string with a conical deficit). As a result, massive particles will experience a new attractive force $F \propto (\mu - T)/v_s$, where v_s is the string velocity [17]. At the same time, the propagation of photons in a plane perpendicular to the string is unaffected by the rod-like feature of the wiggly string metric and is only affected by the conical deficit. This fact—that the effect of wiggleness on massive particles is qualitatively different from the effect on radiation—seems especially relevant when calculating CMBR anisotropy and the power spectrum. It may be hoped that this feature could help alleviate the current difficulties in reconciling the Cosmic Background Explorer (COBE) normalized matter power spectrum with the observational data in the cosmic string model.

It should be pointed out that the model we have adopted cannot be the final word since a number of factors have still not been taken into account. In the network itself, the infinite strings will produce loops which will then decay by emitting gravitational radiation. The effect of the loops is only included insofar that they can be treated as segments of strings. In other words, large loops are included in our analysis but small loops have been missed. Also, the decay of loops into gravitational radiation has been missed. The back reaction of gravitational radiation on the string segments is completely neglected. We hope to rectify some of these omissions by further modeling of the network in subsequent work.

In the following sections we use the model developed in Ref. [2] to calculate the CMBR anisotropy and the matter power spectrum due to cosmic strings in a few cosmologies. The energy-momentum tensor that we use is that of wiggly strings, as we describe in the next section. In addition, the characteristics of the string network (velocity and correlation length) are computed using the one-scale model described in Sec. III. There are some further assumptions that we have to make about the string network that we also describe in this section. Our results for the CMBR anisotropy and the power spectrum in density inhomogeneities for a few different cosmologies are given in Sec. IV. Here we also discuss the model dependence of our results. Our conclusions are summarized in Sec. V.

II. WIGGLY STRINGS

The world history of a string can be represented by a two-dimensional surface in spacetime,

$$x^\mu = x^\mu(\zeta^a), \quad a = 0, 1,$$

called the string world sheet, where ζ^0 and ζ^1 are the coordinates on the world sheet.

We consider strings that reside in an expanding universe described by the metric

$$ds^2 = a^2(\tau)(d\tau^2 - d\mathbf{x}^2),$$

where τ is the conformal time. The string equations of motion are invariant under reparametrization of the string world sheet. A convenient choice of the parametrization (gauge) is

$$\zeta^0 = \tau, \quad \mathbf{x}' \cdot \dot{\mathbf{x}} = 0,$$

where the prime denotes a derivative with respect to ζ^1 . In this gauge the energy-momentum tensor of a string is

$$T^{\mu\nu}(y) = \frac{\mu}{\sqrt{-g}} \int d^2\zeta (\epsilon \dot{x}^\mu \dot{x}^\nu - \epsilon^{-1} x'^\mu x'^\nu) \delta^{(4)}(y - x(\zeta)), \quad (1)$$

where $\sigma = \zeta^1$ and

$$\epsilon = \sqrt{\frac{\mathbf{x}'^2}{1 - \dot{\mathbf{x}}^2}}. \quad (2)$$

Following Carter [15] we can define the string tension T and the string mass-energy per unit length U by

$$\sqrt{-g} T^{\mu\nu}(y) = \int d^2\zeta \sqrt{-\gamma} (U u^\mu u^\nu - T v^\mu v^\nu) \delta^{(4)}(y - x(\zeta)), \quad (3)$$

where u^μ and v^μ are such that

$$u_\mu u^\mu = -v_\mu v^\mu = 1, \quad u_\mu v^\mu = 0, \quad (4)$$

$$(u^\mu v^\rho - v^\mu u^\rho)(u_\rho v_\nu - v_\rho u_\nu) = \eta_\nu^\mu, \quad (5)$$

$$\eta^{\mu\nu} = \gamma^{ab} x_{,a}^\mu x_{,b}^\nu, \quad (6)$$

and γ^{ab} is the world sheet metric. One can check that

$$u^\mu = \frac{\sqrt{\epsilon} \dot{x}^\mu}{(-\gamma)^{1/4}}, \quad v^\mu = \frac{x'^\mu}{\sqrt{\epsilon} (-\gamma)^{1/4}} \quad (7)$$

satisfy the conditions (4)–(6). Substituting Eqs. (7) into Eq. (1) and comparing with Eq. (3) one obtains

$$U = T = \mu, \quad (8)$$

which is the equation of state for an ordinary (“intrinsically isotropic” [15]) Nambu-Goto string [18].

Lattice simulations of string formation and evolution suggest that strings are not straight but have wiggles [8]. A distant observer, however, would not be able to resolve the small-scale structure. Instead, he would see a smooth string with the effective mass per unit length \tilde{U} and the tension \tilde{T} . The equation of state for a wiggly string averaged over the small-scale structure has been shown [15,16] to be

$$\tilde{U} \tilde{T} = \mu^2 \quad (9)$$

or

$$\tilde{U} = \alpha\mu, \quad \tilde{T} = \mu/\alpha, \quad (10)$$

where $\alpha = \alpha(\sigma, \tau)$ is, in general, some function of time and the coordinate along the length of the smoothed string. The energy-momentum tensor of a wiggly string viewed by an observer who cannot resolve the wiggly structure is then obtained by substituting Eqs. (10) into Eq. (3):

$$\begin{aligned} \tilde{T}^{\mu\nu}(y) &= \frac{1}{\sqrt{-g}} \int \frac{d^2\zeta}{\sqrt{-\gamma}} (\tilde{U} u^\mu u^\nu - \tilde{T} v^\mu v^\nu) \delta^{(4)}(y - x(\zeta)) \\ &= \frac{\mu}{\sqrt{-g}} \int d^2\zeta \left[\epsilon \alpha \dot{x}^\mu \dot{x}^\nu - \frac{x'^\mu x'^\nu}{\epsilon \alpha} \right] \delta^{(4)}(y - x(\sigma, \tau)). \end{aligned}$$

Next, we use this expression to calculate the stress-energy of a string network.

III. STRING NETWORK

A. Parameters of the network

The string network at any time can be characterized by a single length scale, the correlation length L , defined by

$$\rho = \frac{\mu}{L^2}, \quad (11)$$

where ρ is the energy density in the string network. It will be convenient to work with the comoving correlation length $l = L/a$.

The expansion stretches the strings, thus increasing the energy density. At the same time, long strings reconnect and chop off loops which later decay. The evolution of l including only these two competing processes is [13,14,19]

$$\frac{dl}{d\tau} = \frac{\dot{a}}{a} l v^2 + \frac{1}{2} \tilde{c} v \quad (12)$$

$$\frac{dv}{d\tau} = (1 - v^2) \left(\frac{\tilde{k}}{l} - 2 \frac{\dot{a}}{a} v \right), \quad (13)$$

where v is the rms string velocity, \tilde{c} is the loop chopping efficiency and \tilde{k} is the effective curvature of the strings. The values of \tilde{c} and \tilde{k} in radiation and matter eras are suggested in [19]. We use the same scheme as in Ref. [3] to interpolate between these values through the radiation-matter transition:

$$\tilde{c}(\tau) = \frac{c_r + g a c_m}{1 + g a}$$

$$\tilde{k}(\tau) = \frac{k_r + g a k_m}{1 + g a},$$

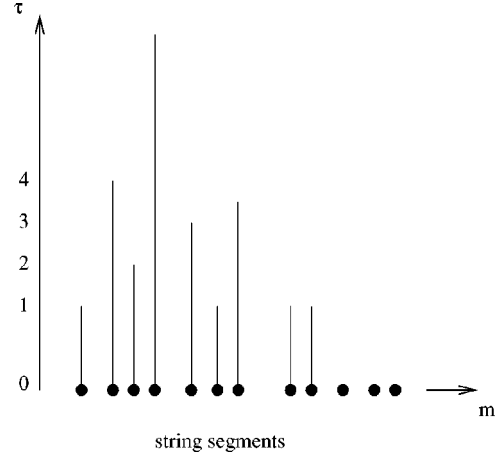


FIG. 1. A schematic picture of the string network model. All string segments (depicted by solid circles) are born at an early epoch and then decay at various later times. The segments are labeled by the index m and the decay times are shown as numbers along the τ axis. In certain cosmologies, it is possible that some string segments never decay.

where we take $c_r = 0.23$, $c_m = 0.18$, $k_r = 0.17$, $k_m = 0.49$, $g = 300$ and $a(\tau)$ is normalized so that $a = 1$ today.¹

B. Model of the network

Here we closely follow the model described in [2,3].

The basic picture is that the string network is represented by a collection of uncorrelated, straight string segments moving with random, uncorrelated velocities. All the segments are assumed to be produced at some early epoch. At every subsequent epoch, a certain fraction of the number of segments decay in a way that maintains network scaling. This picture of the network is depicted in Fig. 1.

The comoving length, l , of each segment at any time is taken to be equal to the correlation length of the network defined below Eq. (11). The positions of the segments are drawn from a uniform distribution in space and their orientations are chosen from a uniform distribution on a two sphere. The segment speeds are fixed to be given by the solution of Eq. (13) while the direction of the velocity is taken to be uniformly distributed in the plane perpendicular to the string orientation.² In principle, this constraint on the velocity does not remain valid when the strings are wiggly since the wiggles can impart a longitudinal velocity to the segments. However, as explained below, the longitudinal velocities are expected to be much smaller than the transverse velocities and hence will be neglected.

¹This choice of the value of g along with our normalization for a leads to the same time dependence of v and l as in [3]. Normalizing a so that $a = 1$ at equality would require a much smaller value, e.g. $g \sim 0.1$, as reported in [3].

²We have also performed a few simulations where we drew the velocities from a Gaussian distribution as in Ref. [2], but these did not lead to significantly different results.

The decay of segments of the string network is accomplished by ‘‘turning off’’ the energy-momentum of a fraction of the existing segments at every epoch. Each segment is assigned a certain decay time, τ_m , where the index m labels the individual segments. So the Fourier transform of the total stress-energy of the network is the sum over the stress-energies of all segments:

$$\Theta_{\mu\nu}(\vec{k}, \tau) = \sum_{m=1}^{N_0} \Theta_{\mu\nu}^m(\vec{k}, \tau) T^{\text{off}}(\tau, \tau_m), \quad (14)$$

where N_0 is the initial number of segments, and $T^{\text{off}}(\tau, \tau_m)$ is a smooth function that turns off the m^{th} string segment by time τ_m .³ The functional form is taken to be [2]

$$T^{\text{off}}(\tau, \tau_m) = \begin{cases} 1 & \dots \tau < L\tau_m, \\ \frac{1}{2} + \frac{1}{4}(x^3 - 3x) & \dots L\tau_m < \tau < \tau_m, \\ 0 & \dots \tau > \tau_m, \end{cases} \quad (15)$$

where

$$x = 2 \frac{\ln(L\tau_m/\tau)}{\ln(L)} - 1 \quad (16)$$

and $L < 1$ is a parameter that controls how fast the segments decay.

The total energy of the string network in a volume V at any time is

$$N\mu L = V\rho = \frac{\mu V}{L^2} \quad (17)$$

where $N = N(\tau)$ is the total number of string segments at that time, $V = V_0 a^3$, $a = 1$ at the present epoch and V_0 is a constant simulation volume. From Eq. (17) it follows that

$$N = \frac{V}{L^3} = \frac{V_0}{l^3}. \quad (18)$$

The comoving length l is approximately proportional to the conformal time τ and implies that the number of strings $N(\tau)$ within the simulation volume V_0 falls as τ^{-3} . To calculate the CMB anisotropy we need to evolve the string network over at least four orders of magnitude in cosmic expansion. Hence we would have to start with $N \gtrsim 10^{12}$ string segments in order to have one segment left at the present time. This is the main problem in directly dealing with the expression for the energy-momentum tensor in Eq. (14).

A way around this difficulty was suggested in Ref. [2]. The suggestion is to consolidate all string segments that de-

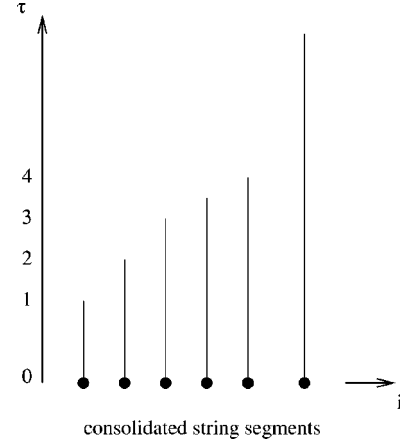


FIG. 2. The modified model of the string network. All strings that decay at the same (discretized) time in Fig. 1 are consolidated into one string segment and assigned a weight that is the square root of the number of segments that the consolidated segment represents. This works for all segments that decay by the end of the simulation but will miss those segments that do not decay. In the present scheme, the segments that will not have decayed by the end of the simulation are consolidated into one string. The contribution of this surviving segment is the remainder term in the expression for the energy-momentum tensor in Eq. (20).

decay at the same epoch. Since the number of segments that decay at the (discretized) conformal time τ_i is

$$N_d(\tau_i) = V[n(\tau_{i-1}) - n(\tau_i)] \quad (19)$$

where $n(\tau)$ is the number density of strings at time τ , the ‘‘consolidated string’’ decaying at τ_i is taken to have weight: $\sqrt{N_d(\tau_i)}$. (The assumption is that string segments that decay at the same time act randomly, leading to the square root in the weight). The number of consolidated strings is of the order of a few hundred and can be dealt with computationally.⁴ This modified picture of the string network is shown in Fig. 2.

Now we can choose τ_n to be equally spaced on a logarithmic scale between τ_{\min} and τ_{\max} and write the energy-momentum tensor as

$$\Theta_{\mu\nu}(\vec{k}, \tau) = \sum_{i=1}^K [N_d(\tau_i)]^{1/2} \Theta_{\mu\nu}^i(\vec{k}, \tau) T^{\text{off}}(\tau, \tau_i) + \mathcal{T}_{\mu\nu} \quad (20)$$

where K is the number of consolidated segments and $\mathcal{T}_{\mu\nu}$ is a remainder that we have included and that we now explain.

The sum in Eq. (20) misses any string segments that have not decayed by τ_{\max} . The remainder $\mathcal{T}_{\mu\nu}$ is supposed to represent the contribution of these segments of strings. As in the

³In addition, Albrecht *et al.* introduce a function T^{on} which turns on the segments at a very early time. This function is not a feature of the model but only introduced to speed up the code. We have not included T^{on} in our simulations.

⁴In addition to consolidating the string segments decaying at a given time into a single ‘‘consolidated string’’ we have also tried consolidating them into two, three and four strings. This did not lead to any difference in the final results.

case of the decaying strings, we will consolidate these surviving segments into one segment with the weight $\sqrt{Vn(\tau_{\max})}$. Therefore

$$\mathcal{T}_{\mu\nu} = \sqrt{Vn(\tau_{\max})} \Theta_{\mu\nu}^{(1)}(\vec{k}, \tau) \quad (21)$$

where the superscript on Θ means that it is the energy-momentum tensor for one string segment.

For certain cosmologies—those without a cosmological constant—the remainder term can be made arbitrarily small by choosing a large enough τ_{\max} . This is because $n(\tau) \propto l(\tau)^{-3}$, where $l(\tau) \sim \tau$ is the comoving correlation length, and hence $n(\tau) \rightarrow 0$ as $\tau \rightarrow \infty$. However, if the cosmological constant is non-zero, the universe enters an inflationary epoch and the range of the conformal time is finite, $\tau \in [0, \tau_\infty]$, and given by

$$\tau_\infty = \int_0^{\tau_\infty} d\tau = \int_0^\infty \frac{dt}{a(t)}.$$

In this model, the number density of string segments is assumed to only depend on the correlation length as $n(\tau) \propto l(\tau)^{-3}$. However, the decay of string segments as described by the function T^{off} prevents this relationship from being exact. Instead we have

$$n(\tau) = \frac{C(\tau)}{l(\tau)^3}.$$

The function $C(\tau)$ is determined by requiring that the total number of strings at any time be still given by $V/l(\tau)^3$. Therefore

$$\frac{1}{l(\tau)^3} = \sum_{i=1}^K [n(\tau_{i-1}) - n(\tau_i)] T^{\text{off}}(\tau, \tau_i) + n(\tau_{\max}),$$

and $l(\tau)$ is determined from the one-scale model [Eq. (12)]. [Note that $C(\tau)$ is contained in $n(\tau)$]. It is reassuring to see that the function $C(\tau)$ that we obtain from our code is nearly constant and of order unity throughout the simulation.

The Fourier transform of the energy-momentum tensor of an individual string segment is

$$\begin{aligned} \Theta_{\mu\nu}(\vec{k}, \tau) &= \int d^3x e^{i\vec{k}\cdot\vec{x}} \Theta_{\mu\nu} \\ &= \mu \int_{-l/2}^{l/2} d\sigma e^{i\vec{k}\cdot\vec{X}} \\ &\quad \times \left(\epsilon \alpha \dot{X}^\mu \dot{X}^\nu - \frac{1}{\epsilon \alpha} X'^\mu X'^\nu \right) \end{aligned} \quad (22)$$

where $X^\mu(\sigma, \tau)$ are the coordinates of the segment:

$$X^0 = \tau, \quad \vec{X} = \vec{x}_0 + \sigma \hat{X}' + v\tau \hat{X}, \quad (23)$$

where \vec{x}_0 is the random location of the center of mass, \hat{X}' and \hat{X} are randomly oriented unit vectors satisfying $\hat{X}' \cdot \hat{X} = 0$ and v is the velocity of the string.

The random location vectors, \vec{x}_0 , appear only in the dot product $\vec{x}_0 \cdot \vec{k}$. Instead of generating \vec{x}_0 at random, Albrecht *et al.* generate $\vec{x}_0 \cdot \vec{k}$ for each segment as a random number from $[0, 2\pi]$. We have also followed this scheme.⁵

As mentioned earlier, we will be ignoring the longitudinal velocities of the segments. This is the constraint $\hat{X}' \cdot \hat{X} = 0$ that we have imposed. The justification is that there are on the order of 10^4 left- and right-moving wiggles on a segment of string, each traveling with a velocity of about the speed of light. The average momentum of this ‘‘gas’’ of wiggles will be zero but there can be fluctuations which will lead to a velocity $\sim 1/\sqrt{10^4}$. Such longitudinal velocities are insignificant compared to the transverse velocity expected to be ~ 0.1 .

The differential equations which describe the metric perturbations produced by $\Theta_{\mu\nu}(\vec{k}, \tau)$ do not depend on the direction of \vec{k} . Therefore, without any loss of generality we will assume $\vec{k} = \hat{k}_3 k$ in Eq. (22).

Substituting Eqs. (23) into Eq. (22), integrating over σ and taking the real part gives

$$\Theta_{00} = \frac{\mu\alpha}{\sqrt{1-v^2}} \frac{\sin(k\hat{X}'_3 l/2)}{k\hat{X}'_3/2} \cos(\vec{k} \cdot \vec{x}_0 + k\hat{X}_3 v\tau), \quad (24)$$

$$\Theta_{ij} = \left[v^2 \hat{X}_i \hat{X}_j - \frac{(1-v^2)}{\alpha^2} \hat{X}'_i \hat{X}'_j \right] \Theta_{00}. \quad (25)$$

Θ_{0i} can be found from the covariant conservation equations $\nabla^\mu \Theta_{\mu\nu} = 0$. Here we have assumed that the entire string energy is in long strings. The conservation is violated if one includes the energy in loops and the gravitational radiation. A detailed discussion of this issue can be found in [4].

C. Evolution of parameters

The evolution of the velocity, v , with time is found by solving Eqs. (12) and (13) with a range of possible initial conditions. In Fig. 3 we show the evolution of the string velocity for the initial conditions: $l(\tau_{\min}) = 0.13\tau_{\min}$, $v_0(\tau_{\min}) = 0.65$ for two different cosmological models. Similarly we show the behavior of $l(\tau)/\tau$ as a function of τ in Fig. 4.

The values of the ‘‘wiggleness’’ parameter α have been estimated [8] in the radiation and matter eras to be $\alpha_r \approx 1.9$ and $\alpha_m \approx 1.5$ respectively. In the case of a non-zero cosmological constant, the exponential expansion of the Universe will stretch and smooth out the wiggles, so that $\alpha \rightarrow 1$ in the Λ -dominated epoch. A function that fits the expected evolution of α is (Fig. 5)

⁵In ongoing work, one improvement of the model that we are investigating is a scheme in which we choose $k_{\min} \vec{x}_0 \cdot \hat{k}$ at random in the interval $[0, 2\pi]$ and then multiply by k/k_{\min} where k_{\min} is the smallest wave vector considered in the simulation.

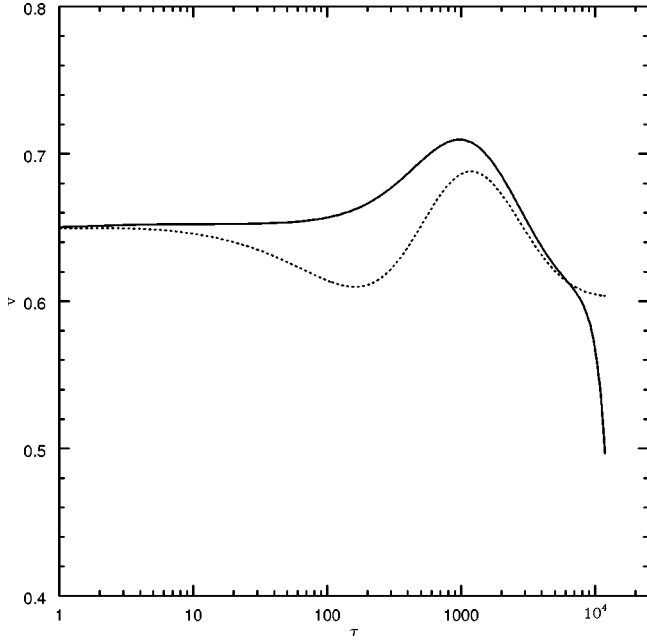


FIG. 3. The velocity of strings v as a function of the conformal time for $\Omega_{baryons}=0.05$, $\Omega_{CDM}=0.95$, $\Omega_{\Lambda}=0$ (dotted line) and $\Omega_{baryons}=0.05$, $\Omega_{CDM}=0.25$, $\Omega_{\Lambda}=0.7$ (solid line).

$$\alpha(\tau) = 1 + \frac{(\alpha_r - 1)a}{\tau \dot{a}}. \quad (26)$$

We shall assume this behavior of α in the next section.

Next, we use the expression for the string stress-energy to calculate the radiation and matter perturbation spectra at present time.

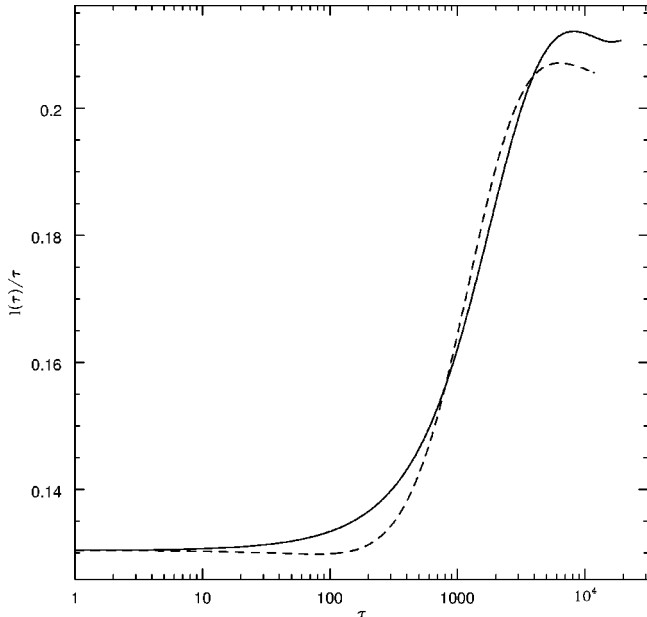


FIG. 4. The length of string segments, $l(\tau)$, divided by τ as a function of τ for $\Omega_{baryons}=0.05$, $\Omega_{CDM}=0.95$, $\Omega_{\Lambda}=0$ (dotted line) and $\Omega_{baryons}=0.05$, $\Omega_{CDM}=0.25$, $\Omega_{\Lambda}=0.7$ (solid line).

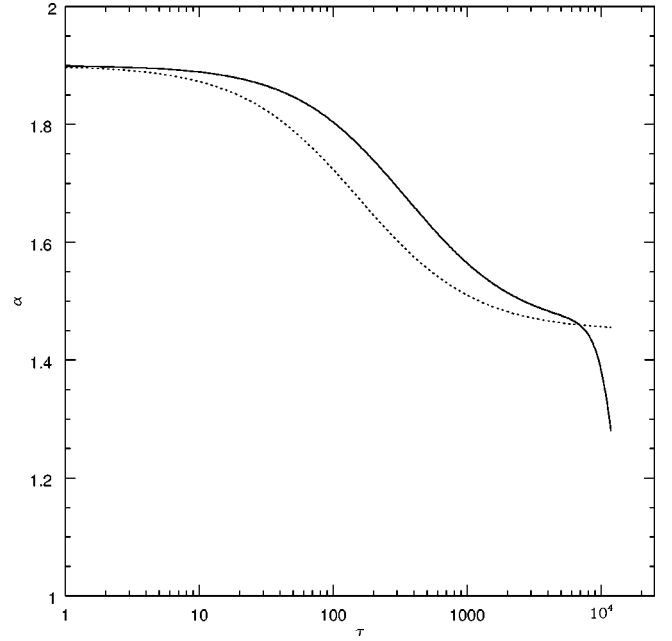


FIG. 5. The wiggleness α as a function of the conformal time for $\Omega_{baryons}=0.05$, $\Omega_{CDM}=0.95$, $\Omega_{\Lambda}=0$ (dotted line) and $\Omega_{baryons}=0.05$, $\Omega_{CDM}=0.25$, $\Omega_{\Lambda}=0.7$ (solid line).

IV. RESULTS

We calculate the CMB anisotropy using the line of sight integration approach [7] implemented in the publicly available code CMBFAST. Given $\Theta_{\mu\nu}$ for each k and τ , CMBFAST integrates the Einstein equations simultaneously with the Boltzmann equations for all radiation and matter particles present in the model. Two factors that have not been included in our analysis are (1) compensation of string inhomogeneities by perturbations in the matter fluids and (2) small loops of string. The first factor was considered in Ref. [2] which we are closely following. However, it was found there that the effects of compensation do not significantly alter the predictions of anisotropy and power spectrum. It is possible that the second factor is important. At the moment, we do not have a good model for including loops in our analysis as there is not much information available in the literature on which to build such a model. The inclusion of loops in the model is a problem that we postpone for the future, though the slow decay of string segments described below may mimic the presence of loops to some extent.

The CMBR anisotropy as seen by an observer can be described by $\Delta(\mathbf{x}, \hat{n}, \tau_0) \equiv |T(\mathbf{x}, \hat{n}, \tau_0) - \bar{T}|/\bar{T}$, where \mathbf{x} is the position of the observer, \hat{n} is the line of sight direction, τ_0 is the conformal time today and \bar{T} is the average temperature of CMBR. At $\mathbf{x}=0$ one can decompose Δ into spherical harmonics

$$\Delta(\hat{n}) = \sum_{lm} a_{lm} Y_{lm}(\hat{n}). \quad (27)$$

The angular power spectrum C_l is defined by

$$C_l \equiv \frac{1}{2l+1} \sum_{m=-l}^l \langle a_{lm}^* a_{lm} \rangle, \quad (28)$$

where $\langle \rangle$ denotes an ensemble average. A self-consistent treatment of the line of sight method and the complete set of the equations are given in [20]. The output of CMBFAST is the COBE normalized angular power spectrum of temperature anisotropy and the power spectra of each of the matter species that is present.

In its current version CMBFAST calculates perturbations from scalar and tensor sources. Since strings may generate a significant vector component, we had to add the vector part to the code.⁶

Our results for the anisotropy and power spectrum are averages over M different realizations of a random network of strings. In the limit of large M , each quantity that we calculate will have an associated probability distribution. For example, for each l the distribution of C_l will approach some probability function with mean \bar{C}_l and standard deviation σ_l . For the averaged result, \bar{C}_l , the standard deviation is σ_l/\sqrt{M} . Performing a large number of experiments on a computer allows us to find \bar{C}_l and σ_l quite accurately. However, an observer (e.g. COBE) trying to determine \bar{C}_l would only be able to average over $(2l+1)$ causally disconnected patches on the sky. Therefore, the accuracy in determining \bar{C}_l observationally is $\sigma_l/\sqrt{2l+1}$. We take this limitation (known as ‘‘cosmic variance’’) into account when plotting the 1σ -error bars on our graphs.

Our results were found by averaging over $M=300$ string network realizations; however, 100 runs would be enough to reproduce most of our results. The simulation with 100 runs took about 10 h to run on a single processor IBM 590 workstation and about 5 h on 10 processors of the J90 cluster of the National Energy Research Scientific Computing Center.

We work only with a flat universe with and without a cosmological constant. We consider two cases ($\Omega_{baryons}=0.05$, $\Omega_{CDM}=0.95$, $\Omega_\Lambda=0$) and ($\Omega_{baryons}=0.05$, $\Omega_{CDM}=0.25$, $\Omega_\Lambda=0.7$). The first case is what until recently was known as the standard CDM model. The second is motivated by the recent supernova data that suggest $\Omega_\Lambda=0.7$ and a flat universe. The value of the Hubble constant in both cases was taken to be $H_0=50 \text{ km sec}^{-1} \text{ Mpc}^{-1}$.

In Fig. 6 we show the effect that wiggleness has on C_l 's for the case when $\Omega_\Lambda=0$ along with the compiled experimental data [21]. The matter power spectrum for the same set of parameters is shown in Fig. 7 together with the data from surveys of galaxies and clusters of galaxies [22]. Adding wiggleness results in a higher peak at $l \approx 400$. However, it does not improve the shape or the magnitude of the matter power spectrum which appears to be in disagreement with data. The COBE normalization allows us to determine the string mass per unit length. We obtain that $G\mu_0$

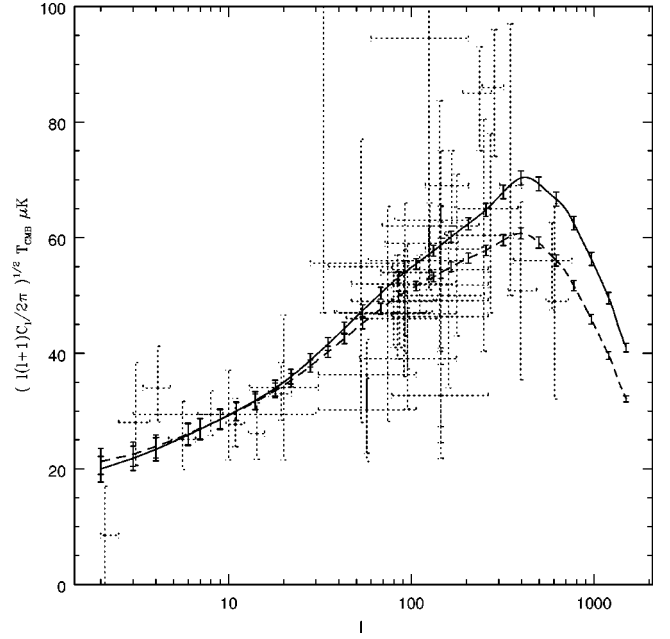


FIG. 6. The total angular power spectrum with (solid line) and without (dashed line) including the wiggleness when $\Omega_{baryons}=0.05$, $\Omega_{CDM}=0.95$, $\Omega_\Lambda=0$ and $v_0=0.65$. The compiled observational data are plotted for comparison.

$=1.1 \times 10^{-6}$ for wiggly strings and $G\mu_0=1.5 \times 10^{-6}$ for smooth strings.

Allowing for a non-zero cosmological constant improves the agreement with the data. In Fig. 8 and Fig. 9 we plot the results of the simulation with $\Omega_\Lambda=0.7$. The peak in the CMBR anisotropy is now higher compared to the $\Omega_\Lambda=0$ case. The power spectrum in Fig. 9 includes the factor of

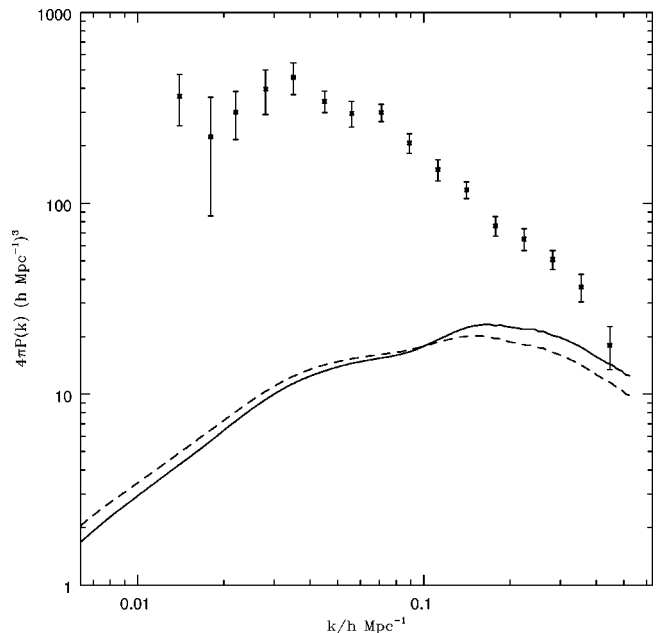


FIG. 7. The matter power spectrum for the same choice of parameters as in Fig. 6. The data extracted from surveys of galaxies and clusters of galaxies are plotted for comparison.

⁶Our code can be downloaded from the website <http://theory4.phys.cwru.edu/~levon>.

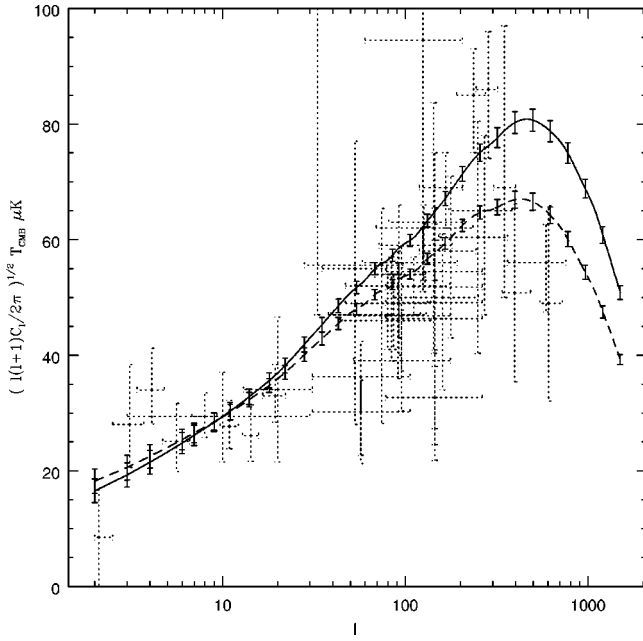


FIG. 8. The total angular power spectrum for wiggly (solid line) and smooth (dashed line) strings when $\Omega_{\text{baryons}}=0.05$, $\Omega_{\text{CDM}}=0.25$, $\Omega_{\Lambda}=0.7$ and $v_0=0.65$.

$\Omega_{\text{matter}}^{0.3}$ necessary for correct comparison with data [22]. Although the magnitude is significantly lower than the data, the shape of the matter power spectrum is improved. The wiggliness results in a higher peak in C_l 's and a slight increase in the magnitude of matter power spectrum at smaller length scales. The string mass per unit length obtained from COBE normalization is practically the same as in $\Omega_{\Lambda}=0$ case.

There is evidence from simulations [8] that the large scale string velocities are much smaller than those plotted in Fig.

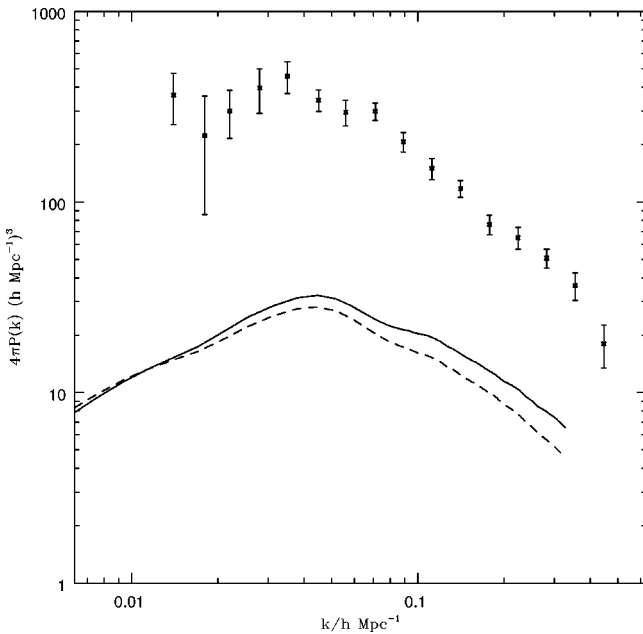


FIG. 9. The matter power spectrum for the same choice of parameters as in Fig. 8.

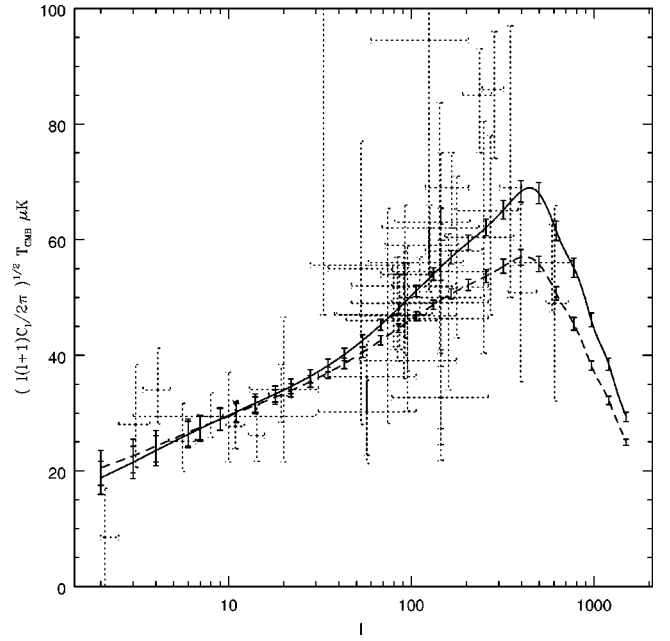


FIG. 10. The total angular power spectrum for wiggly (solid line) and smooth (dashed line) strings when $\Omega_{\text{baryons}}=0.05$, $\Omega_{\text{CDM}}=0.25$ and $\Omega_{\Lambda}=0.7$ and using small values for the string velocities: $v=0.12$ in the radiation era and 0.1 in the matter era.

3. Also, wiggly strings must be heavier and slower than smooth strings because of the different equation of state. We have modified the parameters c_r , c_m , k_r and k_m of the one-scale model in such a way that the rms velocity is 0.12 in the radiation era and 0.1 in the matter era. In Fig. 10 and Fig. 11 we plot the results of using smaller velocities. We see a significant increase in the magnitude of the matter power spectrum. Including the wiggliness results in a slight shift of

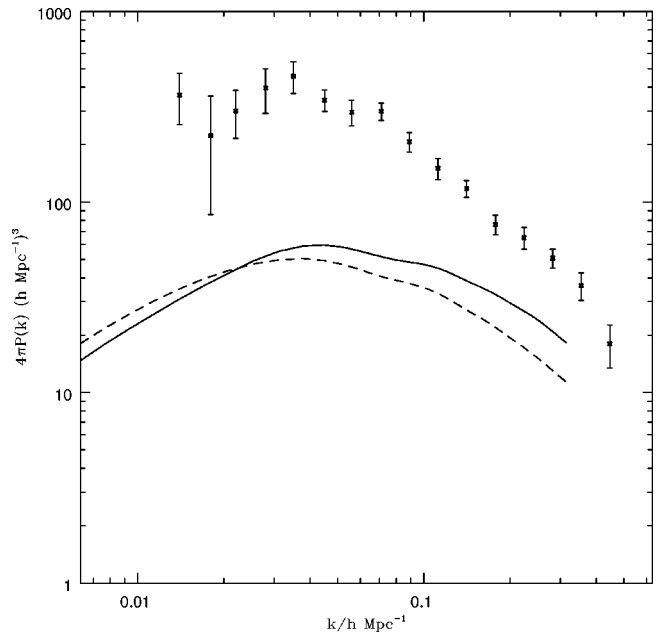


FIG. 11. The matter power spectrum for the same choice of parameters as in Fig. 10.

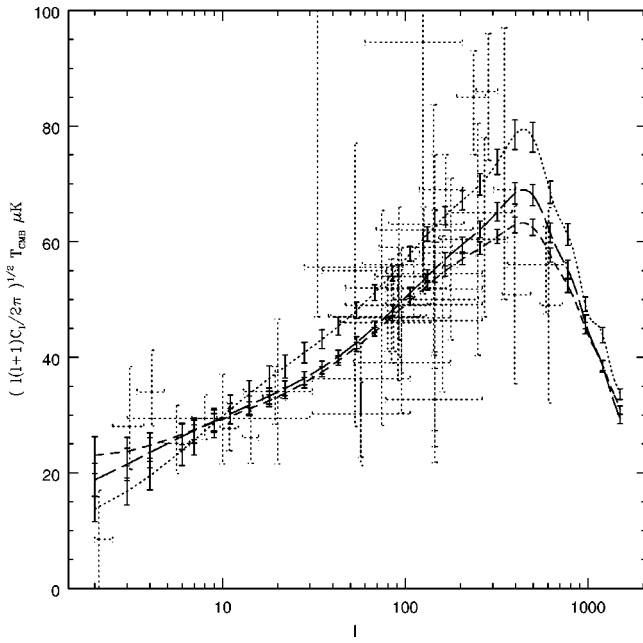


FIG. 12. The total angular power spectrum for the network of wiggly strings with $L=0.1$ (dotted line), $L=0.5$ (long dashed line) and $L=0.92$ (short dashed line). All other parameters are the same as in Fig. 10.

power to smaller scales and an overall increase in magnitude. The scale-dependent bias, required to fit the data, varies between $b \approx 1.6$ on smaller length scales and $b \approx 2.4$ on larger scales. COBE normalization gives $G\mu_0 \approx 2.3 \times 10^{-6}$ for smooth strings and $G\mu_0 \approx 1.9 \times 10^{-6}$ for wiggly strings.

In addition, we have tested the dependence on two other parameters of the model that may have physical significance. These are the string decay rate L and the correlation length of

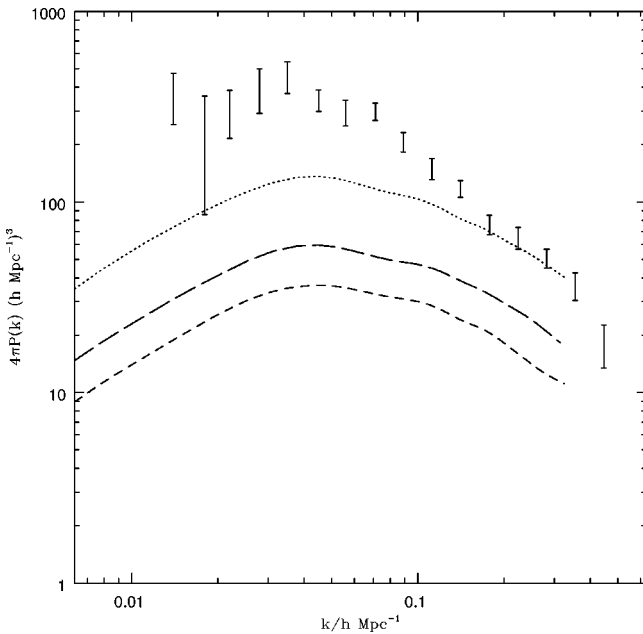


FIG. 13. The matter power spectrum for the same choice of parameters as in Fig. 12.

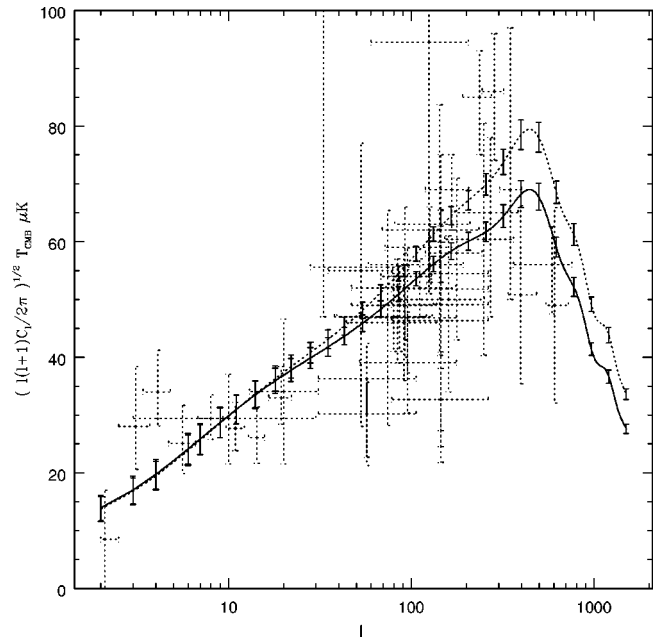


FIG. 14. The total angular power spectrum for the network of wiggly strings with $L=0.1$. The solid line corresponds to the modified $l(\tau)$. The dotted line is the same as in Fig. 13. Other parameters are the same as in Fig. 10.

the network $l(\tau)$. The parameter L appears in the function T^{off} , Eq. (15), and controls how early and how fast the string segments decay. Smaller values of L correspond to an earlier and slower decay. We have used $L=0.5$ for most of our calculations (Figs. 6–11,14,15). In Fig. 12 and Fig. 13 we compare the results of using $L=0.1, 0.5$ and 0.92 . Lower values of L tend to raise the matter power spectrum. When string segments start to decay earlier the effective string den-

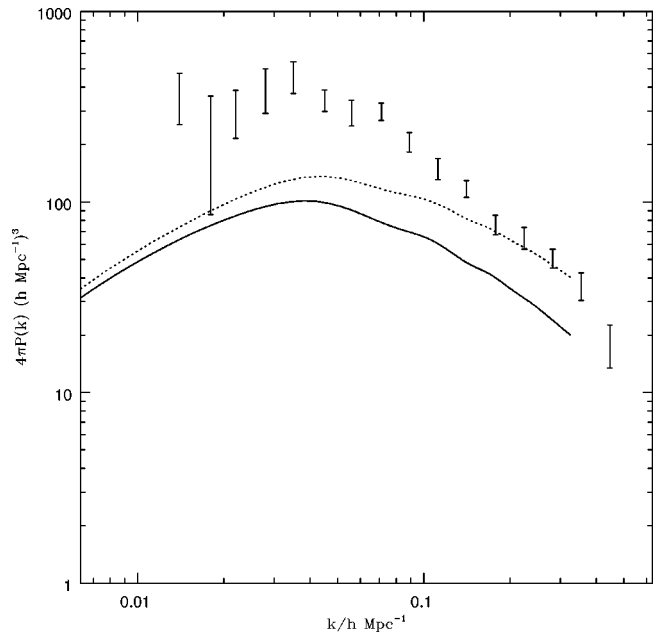


FIG. 15. The matter power spectrum for the same choice of parameters as in Fig. 14.

sity at all times (and especially at later times) will decrease and a larger COBE normalization factor is required to fit the angular power spectrum on large scales. This, of course, increases the value of $G\mu_0$. We obtain $G\mu_0 \approx 4 \times 10^{-6}$ when using $L=0.1$.

The evolution of the correlation length $l(\tau)$ [Eq. (12)] is completely determined by the parameters of the one-scale model, c_r , c_m , k_r and k_m . To obtain the results shown in Figs. 6–13 we have chosen these parameters so that the evolution of $l(\tau)$ is not altered and is the same as in Fig. 4. In Fig. 14 and Fig. 15 we plot the results of the simulation in which the cosmological parameters and the string velocity were taken to be those in Fig. 10 but the parameters of the one-scale model were set to give $l(\tau)/\tau$ equal to 0.24 in the radiation- and 0.3 in the matter-dominated eras. This choice of parameters is largely arbitrary; however, it shows that there is a freedom in the model that may be used to change the shape of the matter power spectrum.

V. CONCLUSIONS

We have seen that including the effects of small-scale structure in the string stress-energy improves the agreement with the observational data. Using $\Omega_\Lambda=0.7$ and reducing the average string velocities gives us a scale-dependent bias factor between 1.6 and 2.4. Allowing for a slower decay rate of strings and larger correlation length of the string network makes the bias factor nearly scale invariant with an average value of 1.9. The scale invariant bias factor of 2 was reported

in [3] which was obtained by introducing an additional time dependence of μ designed to reproduce the shape of the matter power spectrum. The present work has the advantage of not altering the physics of the model.

The one-scale model, Eqs. (12) and (13), is a very coarse approximation of the evolution of wiggly strings. The small-scale structure is included only through the value of the effective curvature $\tilde{\kappa}$, the rest of the equations being exactly the same as for the smooth strings. We expect that a more precise analytical model would improve the agreement with the data. Also, work on improving the model of the string network is in progress as reported in [4] and this should help to eliminate some of the assumptions we have had to make in the present analysis. In addition we are presently investigating ways to relax some of the assumptions of the model described in the paper that will help shed light on the robustness of the predictions.

ACKNOWLEDGMENTS

We would like to thank U. Seljak and M. Zaldarriaga for making CMBFAST available to us and the National Energy Research Scientific Computing Center for the use of their J90 cluster. We are grateful to Martin White for discussion and Julian Borrill for help with supercomputing. We thank Carlos Martins for pointing out the necessity of explaining our choice of the value for g . T.V. was supported by a grant from the U.S. Department of Energy.

-
- [1] U.-L. Pen, U. Seljak, and N. Turok, Phys. Rev. Lett. **79**, 1611 (1997).
 - [2] A. Albrecht, R. Battye, and J. Robinson, Phys. Rev. Lett. **79**, 4736 (1997); Phys. Rev. D **59**, 023508 (1998).
 - [3] R. Battye, J. Robinson, A. Albrecht, Phys. Rev. Lett. **80**, 4847 (1998).
 - [4] C. Contaldi, M. Hindmarsh, and J. Magueijo, Phys. Rev. Lett. **82**, 679 (1999).
 - [5] E.J. Copeland, J. Magueijo, and D.A. Steer, astro-ph/9903174.
 - [6] P.P. Avelino, E.P.S. Shellard, J.H.P. Wu, and B. Allen, Phys. Rev. Lett. **81**, 2008 (1998).
 - [7] U. Seljak and M. Zaldarriaga, Astrophys. J. **469**, 437 (1996).
 - [8] D.P. Bennett and F.R. Bouchet, Phys. Rev. D **41**, 2408 (1990); E.P.S. Shellard and B. Allen, in *Formation and Evolution of Cosmic Strings*, edited by G.W. Gibbons, S.W. Hawking, and T. Vachaspati (Cambridge University Press, Cambridge, England, 1990).
 - [9] D.P. Bennet, F.R. Bouchet, and A. Stebbins, Nature (London) **335**, 410 (1988).
 - [10] B. Allen, R.R. Caldwell, S. Dodelson, L. Knox, E.P.S. Shellard, and A. Stebbins, Phys. Rev. Lett. **79**, 2624 (1997).
 - [11] L. Perivolaropoulos, Phys. Lett. B **298**, 305 (1993); Astrophys. J. **451**, 429 (1995).
 - [12] G. Vincent, M. Hindmarsh, and M. Sakellariadou, Phys. Rev. D **55**, 573 (1997).
 - [13] T.W.B. Kibble, Nucl. Phys. **B252**, 227 (1985); **B261**, 750 (1986).
 - [14] D.P. Bennett, Phys. Rev. D **33**, 872 (1986); **34**, 3592 (1986).
 - [15] B. Carter, Phys. Rev. D **41**, 3869 (1990).
 - [16] A. Vilenkin, Phys. Rev. D **41**, 3038 (1990).
 - [17] T. Vachaspati and A. Vilenkin, Phys. Rev. Lett. **67**, 1057 (1991).
 - [18] A. Vilenkin, Phys. Rep. **121**, 264 (1985).
 - [19] C.J.A.P. Martins and E.P.S. Shellard, Phys. Rev. D **54**, 2535 (1996).
 - [20] W. Hu, U. Seljak, M. White, and M. Zaldarriaga, Phys. Rev. D **57**, 3290 (1998).
 - [21] Max Tegmark's WWW site: <http://www.sns.ias.edu/~max/cmb/experiments.html>.
 - [22] J.A. Peacock and S.J. Dodds, Mon. Not. R. Astron. Soc. **267**, 1020 (1994).